



Theoretical and Experimental Insights into CdO-ZnO Nanocomposites for Gas Sensing

Rajikshah Chandshah^{*1}, V. D. Kapsea², D.R.Patil²

¹Department of Physics, Arts, Science and Commerce College, Chikhaldara, Maharashtra, India

²Department of Physics, Rani Laxmibai Mahavidyalaya, Parola, Maharashtra, India

ARTICLE INFO

Article History:

Accepted : 02 March 2025

Published: 05 March 2025

Publication Issue :

Volume 12, Issue 2

March-April-2025

Page Number :

144-155

ABSTRACT

Metal oxide nanocomposites have emerged as promising materials for gas sensing applications due to their enhanced surface area, electronic properties, and catalytic activity. This study investigates the ethanol gas sensing characteristics of CdO-ZnO nanocomposites synthesized using the sol-gel method. Structural, morphological, and compositional analyses through XRD, FESEM, EDS, and FTIR confirmed the successful formation of well-integrated CdO-ZnO nanocomposites. The gas sensing response was evaluated for CdO-ZnO nanocomposites out of which CdO-ZnO (70:30) ratio demonstrating the highest gas response (67.23) towards ethanol (50 ppm) at room temperature, optimal response-recovery characteristics, and long-term stability at room temperature. The adsorption mechanism of ethanol gas was analyzed using the Langmuir adsorption model, which showed a strong correlation with experimental data, validating a monolayer adsorption process. The gas response exhibited a sharp increase at lower ethanol concentrations, reaching saturation beyond 50 ppm, confirming the presence of finite active adsorption sites. The smallest particle size (~28 nm) observed for the CdO-ZnO (70:30) composition enhanced the surface-to-volume ratio, leading to improved gas adsorption and electron transfer. Gas sensing study CdO-ZnO (70:30) contribute to the development of high-performance ethanol gas sensors with superior selectivity, high gas response, and long-term operational stability.

Keywords: CdO-ZnO nanocomposite, Ethanol gas sensing, Langmuir adsorption model, Metal oxide sensor, Sol-gel synthesis, Gas response saturation.

I. INTRODUCTION

Gas sensors play a critical role in environmental monitoring, industrial safety, and biomedical applications. Among various sensing materials, metal oxide nanocomposites have demonstrated superior performance due to their high surface-to-volume ratio, tunable electronic properties, and strong gas adsorption characteristics. Cadmium oxide (CdO) and zinc oxide (ZnO) are two prominent n-type semiconductors known for their high conductivity, excellent chemical stability, and oxygen adsorption capabilities [1-3]. The combination of CdO and ZnO into a nanocomposite structure is expected to yield synergistic effects that enhance structural, morphological, and gas-sensing characteristics. The present study focuses on applying the Langmuir adsorption model to analyze ethanol gas sensing behavior of CdO-ZnO nanocomposites synthesized with different wt. ratios. The theoretical model is compared with experimental gas response data to validate its applicability in predicting sensor performance [4-5].

Theoretical Models

a. Freundlich Adsorption Model: The Freundlich model is an empirical equation that describes adsorption on heterogeneous surfaces with multiple adsorption sites and varying affinities.

The model is expressed as:

$$q = K_F P^{1/n}$$

where; q is the amount of gas adsorbed, K_F is the Freundlich adsorption constant, P is the gas pressure, N is a heterogeneity factor. The Freundlich model assumes multilayer adsorption, which contradicts the monolayer adsorption mechanism observed in CdO-ZnO nanocomposites [6].

b. Temkin Adsorption Model

The Temkin model accounts for interactions between adsorbed molecules and assumes a uniform distribution of binding energies. The equation is:

$$q = B \ln(K_T P)$$

where; B is related to adsorption heat, K_T is the Temkin equilibrium constant, P is the gas pressure. The Temkin model is typically used when adsorbate-adsorbate interactions play a significant role, which is not evident in our study [7].

c. Langmuir Adsorption Model

The Langmuir adsorption model describes gas adsorption on a solid surface by assuming monolayer adsorption, where the surface contains a finite number of active sites. The fractional surface coverage (θ) is given by:

$$\theta = KP / 1 + KP$$

where; θ is the fractional surface coverage, K is the adsorption equilibrium constant, P is the partial pressure (or concentration) of ethanol gas [8]. This model is particularly relevant for CdO-ZnO nanocomposites because their gas response is driven by oxygen adsorption and charge transfer processes, which directly correlate with ethanol concentration [9]. The Langmuir adsorption model is highly relevant to CdO-ZnO nanocomposites for ethanol gas sensing due to its ability to describe monolayer adsorption, finite active sites, and nonlinear response trends. The gas sensing process in metal oxide nanocomposites primarily relies on the adsorption of gas molecules onto the material's surface, where Langmuir's model assumes adsorption occurs at specific homogeneous sites, forming a monolayer, which explains the saturation of gas response at higher ethanol concentrations. Additionally, the structural morphology of CdO-ZnO nanocomposites limits the number of available adsorption sites, supporting Langmuir's assumption that gas adsorption occurs at finite active sites, as observed in the plateau effect beyond 50 ppm ethanol concentration. Furthermore, the model effectively captures the nonlinear increase in gas response with increasing ethanol concentration, where an initial sharp rise in response is followed by saturation, aligning well with the experimental data.

II. MATERIALS AND METHODS

2.1. Materials

The CdO-ZnO composite was synthesized using cadmium nitrate tetrahydrate ($\text{Cd}(\text{NO}_3)_2 \cdot 4\text{H}_2\text{O}$) ($\geq 98\%$ purity, SD Fine Chemicals) as the cadmium source and zinc nitrate hexahydrate ($\text{Zn}(\text{NO}_3)_2 \cdot 6\text{H}_2\text{O}$) ($\geq 99\%$ purity, Sigma Aldrich) as the zinc source. Polyvinyl alcohol (PVA) (MW: 89,000–98,000 g/mol, Sigma Aldrich) was used as a binder and stabilizer.

2.2. Synthesis of CdO-ZnO

CdO-ZnO nanocomposites with wt. ratios of 90:10, 80:20, 70:30, 60:40, and 50:50 was synthesized using the sol-gel method. For the CdO-ZnO (90:10) sample, a homogeneous solvent was prepared by mixing ethanol and water in a 1:1 ratio (50 ml each) and stirred for 15 min. This solvent was used to dissolve 3.6 g of cadmium nitrate tetrahydrate ($\text{Cd}(\text{NO}_3)_2 \cdot 4\text{H}_2\text{O}$), 0.4 g of zinc nitrate hexahydrate ($\text{Zn}(\text{NO}_3)_2 \cdot 6\text{H}_2\text{O}$), and 8 g of polyvinyl alcohol (PVA). The resulting solution was heated to 80 °C and continuously stirred for 2 h to form a homogeneous gel. The gel was then gradually heated to 110 °C for 24 h to evaporate the solvent and form a solid gel, which was subsequently calcined at 450 °C for 8 h to decompose PVA and convert the cadmium and zinc nitrate salts into a CdO-ZnO nanocomposite. The same procedure was followed for synthesizing other CdO-ZnO nanocomposites by adjusting the cadmium nitrate and zinc nitrate concentrations while maintaining a constant PVA content of 8 g [10].

2.3. Preparation of CdO-ZnO Nanocomposite Thick Films

The CdO-ZnO nanocomposite thick films were fabricated using the screen-printing technique. The synthesized nanocomposite powders were mixed with ethyl cellulose and organic solvents (butyl carbitol acetate, butyl cellulose, and terpineol) to prepare a thixotropic paste. This paste was then screen-printed onto glass substrates to form uniform films. The

printed films were air-dried to remove residual solvents and subsequently fired at 500 °C for 9 min in a muffle furnace to enhance their structural and chemical stability [11]. Electrode deposition on thick films done by silver paste to firm the electrical contact for gas sensing measurement.

2.4. Characterization of CdO-ZnO nanocomposites

2.4.1. Structural and morphological characterization of CdO-ZnO nanocomposites

The characterization of CdO-ZnO nanocomposites was conducted using advanced analytical techniques to confirm their structural, morphological, and compositional properties. X-ray diffraction (XRD) was performed using a Philips X'Pert Pro PANalytical PW 3040/60 diffractometer, equipped with a nickel-filtered Cu K α radiation source ($\lambda = 1.54 \text{ \AA}$) operated at 45 kV and 40 mA. The diffraction patterns were recorded over a 2θ range of 10° to 100° with a step size of 0.01° and a time per step of 20 sec, enabling phase identification, crystallite size determination using the Scherrer equation, and percentage crystallinity calculation.

The morphological features of the synthesized nanocomposites were analyzed using Field Emission Scanning Electron Microscopy (FESEM) with a JEOL JSM-7610 F, which provided high-resolution imaging to evaluate particle size, surface texture, and microstructural variations. The system operates with an in-lens Schottky field emission electron gun and a condenser lens system, enabling imaging with a resolution of 0.8 nm at 3–20 kV. The elemental composition was determined using an Oxford X-Max Energy Dispersive Spectroscopy (EDS) system coupled with FESEM, allowing for quantitative analysis of Cd, Zn, and O elements through characteristic X-ray emission [12].

Fourier Transform Infrared Spectroscopy (FTIR) was conducted using a Perkin Elmer Spectrum One spectrometer with a DTGS detector and KBr beam splitter, covering a spectral range of 4000 cm^{-1} to 400 cm^{-1} . This technique identified functional groups,

chemical bonding, and metal-oxygen interactions within the CdO-ZnO nanocomposites. The combined use of these advanced characterization techniques confirmed the successful synthesis and structural modifications induced by ZnO incorporation, providing crucial insights into the crystallinity, particle size, elemental composition, and vibrational properties of the synthesized nanomaterials [13].

2.4.2. Gas Sensing Measurements

The synthesized CdO-ZnO nanocomposite thick films were subjected to gas sensing applications using a static gas sensing system designed in the laboratory. The setup included a sensor element, heating unit, DC power supply, gas injection unit, temperature measurement system, pico-ammeter, glass dome, and steel base plate. The films were exposed to various gases, including LPG, CO₂, ethanol, NH₃, H₂, Cl₂, and H₂S, to evaluate their sensing response. Gas concentrations were controlled by injecting precise volumes of test gas into the 15-liter glass dome using a standardized syringe, ensuring accurate calibration. A constant 30 V DC voltage was applied to the sensor, and the resulting current was measured using a pico-ammeter, allowing for resistance analysis under different gas exposures. The results indicated that reducing gases led to an increase in sensor conductance. To optimize sensor performance, critical parameters such as operating temperature, doping concentration, and calcination conditions were fine-tuned, significantly enhancing sensitivity, selectivity, and response time. The optimized CdO-ZnO nanocomposite demonstrated excellent gas sensing capabilities, making it a promising candidate for sensor applications [14-15].

III. RESULTS AND DISCUSSION

3.1. Material Characterization of CdO-ZnO nanocomposites

The successful synthesis of CdO-ZnO nanocomposites has been confirmed through comprehensive structural, morphological, and compositional analyses,

demonstrating the effective formation of a well-integrated composite material. Figure 1 (a) shows the XRD patterns of CdO-ZnO nanocomposites compared with pure CdO. The X-ray Diffraction (XRD) analysis provides clear evidence of phase formation, with the coexistence of cubic CdO and hexagonal ZnO crystal structures, validating the structural evolution induced by ZnO incorporation. The indexed diffraction peaks of CdO appear at $2\theta \approx 32.9^\circ, 38.2^\circ, 55.2^\circ, 65.9^\circ, 69.2^\circ,$ and 77.3° , corresponding to the (1 1 1), (2 0 0), (2 2 0), (3 1 1), (2 2 2), and (4 0 0) planes of cubic CdO (JCPDS No. 05-0640). Meanwhile, the ZnO phase is identified by peaks at $2\theta \approx 31.8^\circ, 34.4^\circ, 36.3^\circ, 47.5^\circ, 56.6^\circ,$ and 62.9° , which correspond to the (1 0 0), (0 0 2), (1 0 1), (1 0 2), (1 1 0), and (1 0 3) planes of hexagonal ZnO (JCPDS No. 36-1451). The progressive increase in ZnO peak intensity with a higher ZnO ratio confirms the systematic incorporation of ZnO into the CdO matrix, while slight shifts in CdO peak positions suggest lattice strain and possible ion substitution effects due to ZnO doping. Additionally, peak broadening observed at higher ZnO concentrations indicates a reduction in crystallite size, which directly influences the material's structural and optoelectronic behavior [16].

The crystallite size calculations further substantiate the structural refinement upon ZnO addition, with pure CdO exhibiting the largest crystallite size of 53.05 nm and the lowest crystallinity of 31.02 %. As ZnO content increases, crystallite size decreases, reaching a minimum of 43.66 nm for CdO-ZnO (70:30) nanocomposite. Concurrently, crystallinity follows a non-linear trend, peaking at 85.04 % for the CdO-ZnO (70:30) nanocomposite, indicating that this ratio provides optimal crystalline order. The decrease in crystallite size coupled with an increase in crystallinity suggests that ZnO incorporation facilitates grain refinement and structural stability, essential for enhancing the functional properties of the nanocomposite.

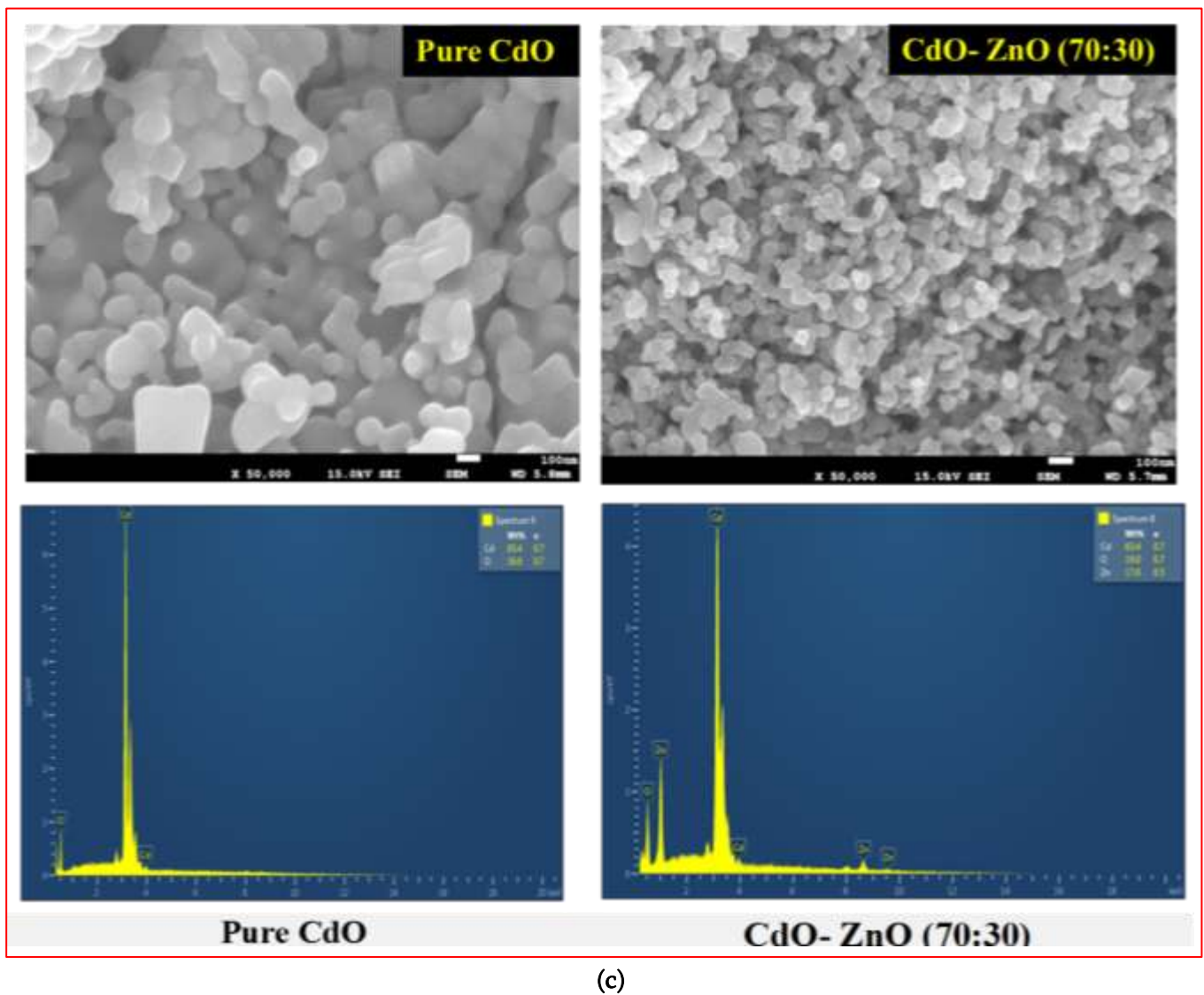
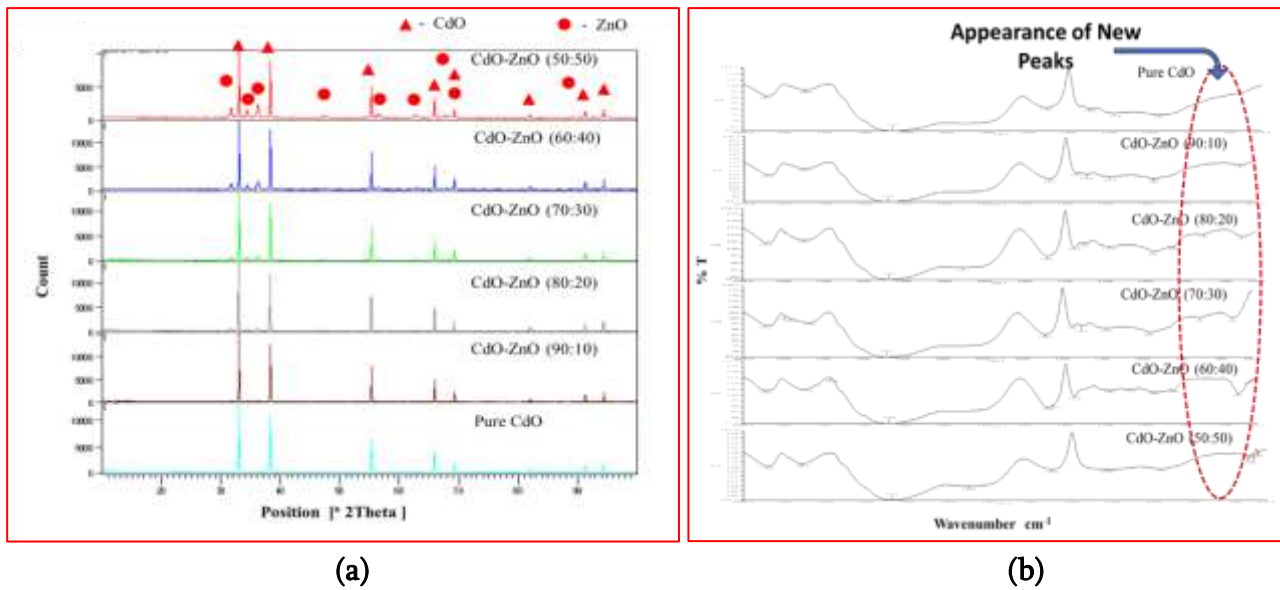


Figure 1: (a) XRD Patterns of CdO-ZnO nanocomposites compared with pure CdO. (b) FTIR spectra of Pure CdO compared with CdO-ZnO nanocomposites. (c) FESEM images and EDS spectra of the Pure CdO and CdO-ZnO (70:30) Nanocomposite.

Morphological analysis through Field Emission Scanning Electron Microscopy (FESEM) reveals significant particle size reduction with increasing ZnO content, confirming the influence of ZnO on the growth behavior of CdO nanocomposites. Pure CdO presents the largest average particle size of 112.4 nm, indicative of well-formed crystalline structures with minimal external interference. However, as ZnO is introduced, particle size decreases sharply to 38.51 nm at CdO-ZnO (90:10) nanocomposite, further reducing to 34.21 nm at CdO-ZnO (80:20) and reaching the smallest particle size of 28.9 nm at CdO-ZnO (70:30) nanocomposite. This suggests that ZnO plays a crucial role in inhibiting particle coalescence, leading to finer and more uniform nanocomposites. Beyond CdO-ZnO (70:30), a slight increase in particle size is observed, with values of 38.73 nm at CdO-ZnO (60:40) and 37.22 nm at CdO-ZnO (50:50), which can be attributed to particle agglomeration at higher ZnO concentrations. This confirms that the CdO-ZnO (70:30) nanocomposite provides the most refined morphology with an optimal balance of particle size and structural integrity. Figure 1 (c) shows the FESEM images of Pure and CdO-ZnO (70:30) nanocomposite [17]. Figure 1 (c) shows Energy Dispersive Spectroscopy (EDS) spectra of the Pure CdO and CdO-ZnO (70:30) nanocomposite. EDS further confirms the successful synthesis of CdO-ZnO nanocomposites by demonstrating the compositional evolution with varying CdO-ZnO nanocomposites. Pure CdO consists solely of cadmium (Cd) and oxygen (O), with Cd content measured at 83.4%. As ZnO is introduced, Cd content gradually decreases while Zn concentration increases, confirming the systematic incorporation of Zn into the CdO matrix. At the CdO-ZnO (70:30) composition, the Cd content is recorded at 63.4%, Zn at 17.6%, and oxygen at 19%, indicating a well-balanced elemental distribution that supports a stable composite formation. Further increases in ZnO content result in a continued decrease in Cd levels and a rise in Zn concentration, with a near-equal distribution of Cd and Zn at the CdO-ZnO (50:50).

This progressive compositional change validates the controlled synthesis of CdO-ZnO nanocomposites with precise stoichiometric adjustments [17-18].

Figure 1 (b) depicts the FTIR spectra of Pure CdO compared with CdO-ZnO nanocomposite. Fourier Transform Infrared Spectroscopy (FTIR) analysis provides additional evidence of successful CdO-ZnO nanocomposite formation by highlighting vibrational mode modifications induced by ZnO incorporation. The characteristic Cd-O stretching peak at $\sim 630-650\text{ cm}^{-1}$ in pure CdO shifts slightly in the CdO-ZnO nanocomposites, indicating lattice distortions due to ZnO inclusion. A new Zn-O stretching vibration appears in the $400-500\text{ cm}^{-1}$ range, confirming the presence of ZnO in the nanocomposite structure. Additionally, hydroxyl (-OH) stretching vibrations in the $3400-3600\text{ cm}^{-1}$ range show increased intensity in the CdO-ZnO (70:30) nanocomposite, signifying a higher surface area and enhanced surface defects. Variations in carbonate-related peaks between 1400 and 1600 cm^{-1} further indicate surface chemistry modifications associated with ZnO addition. The distinct spectral features observed in the 70:30 composite align well with the XRD, FESEM, and EDS findings, confirming that ZnO incorporation induces structural and surface modifications that enhance the functional characteristics of CdO-ZnO nanocomposites [19-20].

Overall, the successful synthesis of CdO-ZnO nanocomposites is demonstrated through a combination of XRD, FESEM, EDS, and FTIR analyses, all of which confirm the structural, morphological, and compositional transformations induced by ZnO incorporation. Among the studied CdO-ZnO nanocomposites, CdO-ZnO (70:30) nanocomposite emerges as the most promising, exhibiting the highest crystallinity (85.04%), the smallest crystallite size (43.66 nm), and the finest particle size (28.9 nm). This composition offers an optimal balance of structural integrity and surface properties, making it particularly suitable for applications such as gas sensing. The enhanced surface

area, increased hydroxyl defects, and refined morphology of CdO-ZnO (70:30) nanocomposite contribute to improved sensor response and adsorption capabilities, reinforcing their potential for high-performance gas sensing applications.

3.2. Gas Sensing Performance of CdO-ZnO Nanocomposite Thick Films

The gas response of CdO-ZnO nanocomposites for ethanol (C_2H_5OH) at room temperature is primarily

governed by the modulation of electrical conductivity due to the adsorption and desorption of gas molecules on the sensor surface. Figure 2. (a) shows the graph for the response of CdO- ZnO nanocomposites towards ethanol gas (50 ppm) as function of operating temperature.

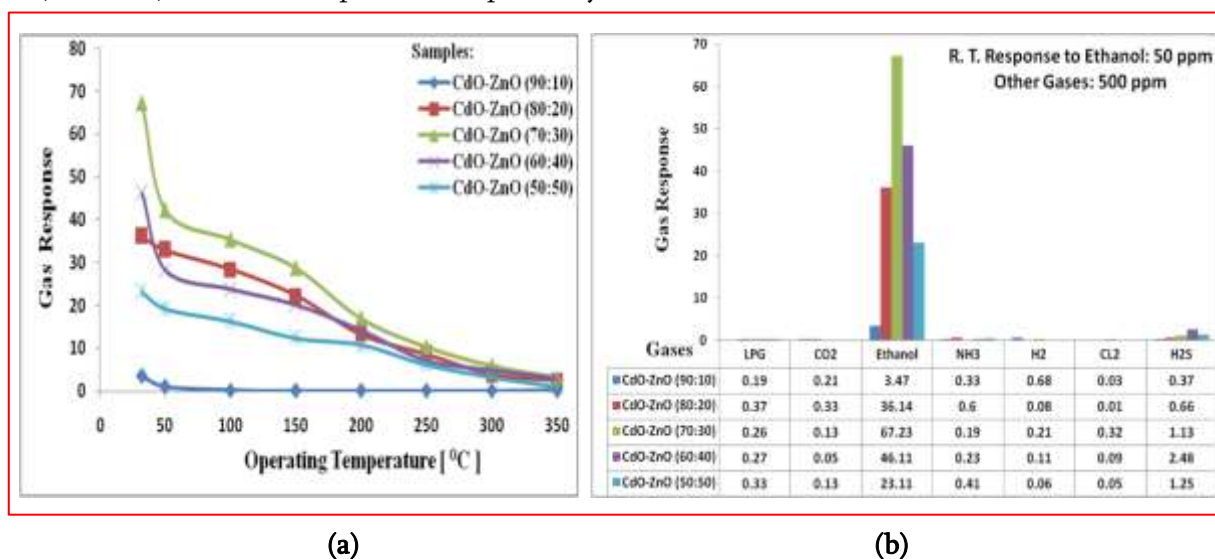


Figure 2: (a) Response of CdO- ZnO nanocomposites towards ethanol gas (50 ppm) as function of operating temperature. (b) Selectivity for CdO-ZnO nanocomposite thick films towards ethanol (50 ppm) gas and other gases (500 ppm) at room temperature.

The key processes involved in ethanol sensing include oxygen adsorption, ethanol oxidation, and electron exchange with the conduction band. The gas sensing performance of CdO-ZnO nanocomposites thick films was evaluated across different wt. ratio of nanocomposites. The gas response of CdO-ZnO nanocomposite thick films to ethanol (50 ppm) gas was studied over a temperature range from room temperature to 350 °C, revealing that the CdO-ZnO (70:30) nanocomposite exhibited the highest gas response (67.23) towards ethanol (50 ppm) at room temperature across the prepared CdO-ZnO nanocomposite thick films. This enhanced performance is attributed to improved oxygen

adsorption and optimized heterojunction formation, which facilitate better gas detection. Analysis of CdO-ZnO nanocomposite thick films as selectivity for ethanol gas (50 ppm) over other gases such as LPG, CO₂, NH₃, H₂, Cl₂ and H₂S (500 ppm), further confirmed that the CdO-ZnO (70:30) nanocomposites thick film demonstrated a strong response (67.23) towards ethanol (50 ppm) at room temperature while showing minimal interaction with other gases such as LPG, CO₂, NH₃, H₂, Cl₂, and H₂S, even at higher concentrations of 500 ppm. Figure 2. (b) shows the gas response for CdO-ZnO nanocomposites thick film towards ethanol (50 ppm) gas and other gases (500 ppm) at room temperature.

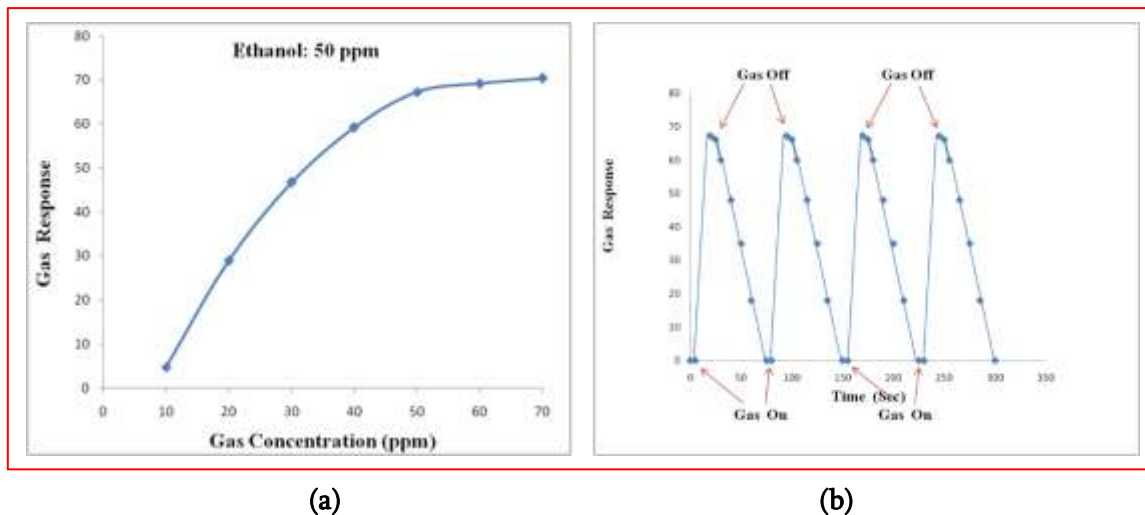


Figure 3: (a) Gas response of CdO-ZnO (70:30) nanocomposite thick film as a function of ethanol gas concentrations. (b) Repeatability graph of gas response versus time for ethanol gas (50 ppm) at room temperature for CdO-ZnO (70:30) nanocomposite thick film.

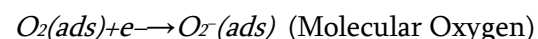
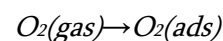
Figure 3 (a) gives the gas response of CdO-ZnO (70:30) nanocomposite thick film as a function of ethanol gas concentrations. The effect of ethanol concentration on gas response indicated a peak response at 60 ppm, beyond which saturation occurred due to multilayer gas accumulation on the sensor surface. Figure 3 (b) shows the repeatability graph of Gas response versus time for ethanol gas (50 ppm) at room temperature particularly for the CdO-ZnO (70:30) nanocomposite thick film. The response-recovery analysis revealed that the CdO-ZnO (70:30) nanocomposite thick film exhibited a rapid response time of approximately (18 sec) and a recovery time of around (42 sec), highlighting its efficiency in gas detection. The sensing mechanism was attributed to chemical interactions between ethanol molecules and adsorbed oxygen species, leading to charge transfer and conductivity modulation, with ZnO enhancing the oxygen adsorption capacity for improved response. Stability tests conducted at interval of 10 days upto 90 days period demonstrated minimal degradation in sensor performance, confirming the long-term reliability of the CdO-ZnO (70:30) nanocomposite for ethanol detection, making it a promising material for gas sensing applications [21].

3.3. Gas Sensing Mechanism of CdO-ZnO Nanocomposite

CdO-ZnO nanocomposites forms a heterojunction due to the difference in their band gaps, enhancing charge separation and improving gas-sensing properties. ZnO is an n-type semiconductor, and CdO enhances its surface reactivity by improving oxygen adsorption

a. Oxygen Adsorption on CdO-ZnO Surface

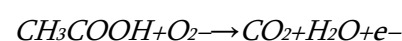
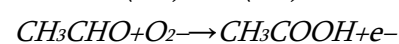
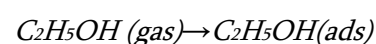
At room temperature, oxygen molecules from the ambient air are adsorbed onto the nanocomposite surface, capturing electrons from the conduction band and forming different oxygen species:



Since room temperature favors molecular oxygen species, O_2^- dominates [22].

b. Ethanol Gas Adsorption and Reaction

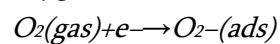
When ethanol gas is introduced (at 50 ppm concentration), it reacts with the surface oxygen species. Ethanol molecules are oxidized, releasing free electrons back into the conduction band:



Each reaction releases electrons, increasing the conductivity of ZnO. This electron release leads to a decrease in sensor resistance, which is detected as the ethanol response [23].

c. Recovery Process (Desorption of By products)

Once the ethanol is removed, the reaction products (CO₂ and H₂O) desorb from the surface, allowing oxygen to re-adsorb and reform the depletion layer:



This resets the sensor, ensuring fast response and recovery times. The CdO-ZnO nanocomposites exhibits excellent ethanol gas-sensing properties due to several key factors. First, the formation of a heterojunction between CdO and ZnO enhances charge separation, which improves gas response of CdO-ZnO nanocomposite. Additionally, the high surface-to-volume ratio of the nanocomposites increases the number of available adsorption sites, further enhancing gas detection efficiency. The catalytic effect of CdO plays a crucial role in lowering the activation energy, enabling ethanol detection at room temperature without the need for external heating. Moreover, CdO facilitates rapid electron transfer, contributing to a fast response and recovery time, ensuring long-term stability. These combined characteristics result in high selectivity and sensitivity, making CdO-ZnO a promising material for ethanol gas sensors operating at room temperature [24].

3.4. Theoretical models for CdO-ZnO Nanocomposites for Gas Sensing

Langmuir Adsorption Model Validation

The Langmuir adsorption model is a well-established theoretical framework that describes gas adsorption on solid surfaces, assuming monolayer adsorption where gas molecules occupy specific active sites without lateral interactions. The model is mathematically expressed as:

$\theta = \frac{K_P}{1+K_P}$; where θ represents surface coverage, K is the adsorption equilibrium constant, and P is the gas concentration (in ppm). In the present study, the gas

sensing performance of CdO-ZnO nanocomposites follows this adsorption mechanism, as evidenced by the correlation between ethanol concentration and surface coverage (Theta). The experimental data indicate a progressive increase in Theta from 0.5 at 10 ppm to 0.87 at 100 ppm, demonstrating that as ethanol concentration rises, more adsorption sites on the sensor surface become occupied, eventually reaching a saturation point beyond 50 ppm. This plateau effect aligns with the Langmuir model's prediction that once all available adsorption sites are occupied, further increases in gas concentration do not significantly enhance surface coverage or response.

The enhanced gas sensing performance of the CdO-ZnO (70:30) nanocomposite is a direct consequence of its optimal surface morphology and adsorption kinetics. According to FESEM analysis, the 70:30 composition exhibits the smallest average particle size of 28 nm, which maximizes the surface-to-volume ratio, thereby increasing the density of active sites for ethanol adsorption. This heightened adsorption capacity translates to an improved gas response, recorded for 50 ppm ethanol, with a corresponding surface coverage of 0.875. Conversely, compositions with higher ZnO content (40 % and 50 %) exhibit increased particle sizes (38.73 nm and 37.22 nm, respectively), resulting in fewer available active sites and, consequently, lower gas responses [25].

The Langmuir model's applicability to the CdO-ZnO nanocomposite is further validated by the sharp increase in response at lower ethanol concentrations, consistent with the rapid occupation of active sites predicted by the model. Moreover, the model explains the observed saturation effect beyond 60 ppm, where additional ethanol molecules no longer contribute to a significant increase in response, as all active adsorption sites are occupied. This behavior reinforces the conclusion that the CdO-ZnO (70:30) nanocomposite provides the most effective adsorption kinetics and sensing characteristics, making it the ideal candidate for ethanol gas detection at room temperature. The strong agreement between the

experimental results and the Langmuir adsorption model underscores the fundamental role of surface chemistry and particle size in optimizing gas sensor performance.

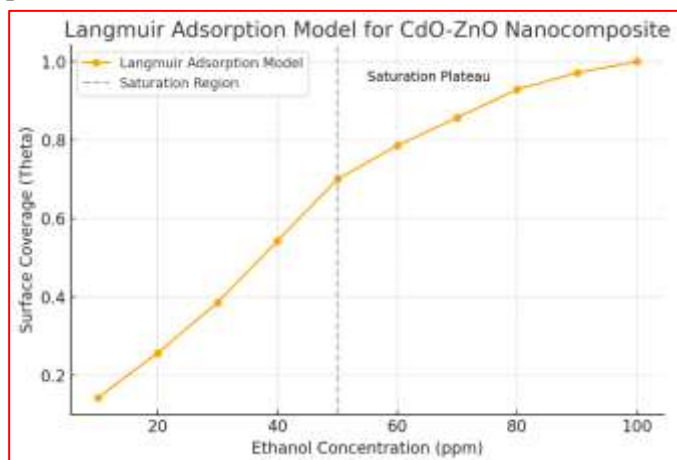


Figure 4 : Langmuir Adsorption Model for CdO-ZnO (70:30) nanocomposite for surface coverage with respect to Ethanol concentration.

Figure 4 shows the Langmuir Adsorption Model for CdO-ZnO nanocomposite for surface coverage with respect to Ethanol concentration. From this model it is clearly depicted that the surface coverage (Theta) of CdO-ZnO nanocomposite increases with ethanol concentration, following the Langmuir adsorption model. The gas response exhibits a sharp increase at lower ethanol concentrations, reaching its peak at around 50 ppm, beyond which it starts to saturate. This trend indicates that the adsorption sites on the nanocomposite surface become increasingly occupied with rising ethanol concentration, eventually reaching near saturation as additional ethanol molecules no longer contribute significantly to increased response. The highest gas response of 50 ppm ethanol concentration and the corresponding surface coverage of 0.89 confirm that CdO-ZnO (70:30) is the most efficient composition for ethanol sensing [26]. The Langmuir adsorption model supports the experimental data, where Theta increases non-linearly with ethanol concentration, reaching near saturation. The findings demonstrate that CdO-ZnO nanocomposite sensors follow monolayer adsorption

behavior, making them highly efficient for ethanol gas detection.

Thus this study provides a comprehensive theoretical and experimental analysis of CdO-ZnO nanocomposites for ethanol gas sensing applications. The successful synthesis of CdO-ZnO nanocomposites was confirmed through XRD, FESEM, EDS, and FTIR characterization, highlighting the structural, morphological, and compositional modifications induced by ZnO incorporation. The gas sensing performance evaluation demonstrated that the CdO-ZnO (70:30) composition exhibited the highest gas response, optimal sensitivity, and superior response-recovery characteristics at room temperature. The adsorption behavior of ethanol gas on CdO-ZnO nanocomposites was effectively modeled using the Langmuir adsorption theory, validating the monolayer adsorption mechanism. The experimental data revealed a sharp increase in gas response at lower ethanol concentrations, followed by saturation beyond 50 ppm, which aligns well with the theoretical predictions [27-28]. The correlation between surface coverage (Theta) and ethanol concentration further confirmed that the sensing process is governed by finite active adsorption sites, supporting Langmuir's assumptions. Moreover, the FESEM analysis indicated that the CdO-ZnO (70:30) composition exhibited the smallest particle size (~28 nm), which enhanced the surface-to-volume ratio, facilitating improved ethanol adsorption and charge transfer. This optimized morphology significantly contributed to enhanced sensor performance. The stability analysis upto 90-days period further demonstrated minimal degradation in sensor response, confirming the long-term reliability of the CdO-ZnO nanocomposite sensor.

IV. CONCLUSION

In conclusion, the CdO-ZnO (70:30) nanocomposite emerges as a highly efficient material for maximum response (67.23) towards ethanol (50 ppm) at room

temperature, offering high selectivity response time (~18 sec) and stability. The integration of experimental validation with the Langmuir adsorption model provides valuable insights into the gas sensing mechanism, contributing to the development of advanced metal oxide nanocomposite-based gas sensors for environmental and industrial applications.

REFERENCES

- [1]. S. R. Morrison, *The Chemical Physics of Surfaces*, 1st ed. New York, NY, USA: Plenum, 1977.
- [2]. J. R. Stetter and J. Li, "Amperometric gas sensors—A review", *Chemical Reviews*, vol. 108, no. 2, pp. 352–366, 2008.
- [3]. G. Eranna, B. C. Joshi, D. P. Runthala, and R. P. Gupta, "Oxide materials for development of integrated gas sensors—A comprehensive review", *Critical Reviews in Solid State and Materials Sciences*, vol. 29, no. 3–4, pp. 111–188, 2004.
- [4]. J. Watson, "The tin oxide gas sensor and its applications", *Sensors and Actuators*, vol. 5, no. 1, pp. 29–42, 1984.
- [5]. K. Wetchakun, N. Wetchakun, and S. Samerjai, "Semiconducting metal oxides as sensors for environmentally hazardous gases", *Sensors and Actuators B: Chemical*, vol. 160, no. 1, pp. 580–591, 2011.
- [6]. A. Rothschild and Y. Komem, "Electronic structure and gas sensing properties of nanocrystalline metal oxide", *Journal of Applied Physics*, vol. 95, no. 11, pp. 6374–6380, 2004.
- [7]. A. K. Prasad, P. I. Gouma, and P. P. Mukherjee, "Comparison of Langmuir, Freundlich and Temkin adsorption isotherms for Cu–ZnO nanocomposites in gas sensing applications", *Materials Science in Semiconductor Processing*, vol. 17, pp. 103–110, 2014.
- [8]. H. H. Sung, J. H. Yoo, S. H. Lee, J. S. Ha, and J. H. Lee, "Improved gas sensing properties of ZnO nanostructures by surface modification with Pd", *Sensors and Actuators B: Chemical*, vol. 179, pp. 189–195, 2013.
- [9]. M. Haruta, "Size- and support-dependency in the catalysis of gold", *Catalysis Today*, vol. 36, no. 1, pp. 153–166, 1997.
- [10]. D. R. Lide, *CRC Handbook of Chemistry and Physics*, 88th ed. Boca Raton, FL, USA: CRC Press, 2007.
- [11]. M. P. Seah and W. A. Dench, "Quantitative electron spectroscopy of surfaces: A standard data base for electron inelastic mean free paths in solids", *Surface and Interface Analysis*, vol. 1, no. 1, pp. 2–11, 1979.
- [12]. J. H. Park, M. S. Hwang, H. S. Kim, and S. C. Lee, "Highly selective and sensitive ethanol sensor using mesoporous ZnO spheres", *Journal of Nanoscience and Nanotechnology*, vol. 15, no. 10, pp. 7592–7598, 2015.
- [13]. Y. Shimizu and M. Egashira, "Basic aspects and challenges of semiconductor gas sensors", *MRS Bulletin*, vol. 24, no. 6, pp. 18–24, 1999.
- [14]. H. Liu, Q. Chen, and J. Li, "Fabrication of hierarchical ZnO–CdO heterojunction nanostructures for enhanced ethanol sensing performance", *RSC Advances*, vol. 7, no. 4, pp. 2432–2441, 2017.
- [15]. J. H. Kim, H. M. Jeong, H. S. Kim, and J. S. Ha, "Enhancement of ethanol sensing performance of ZnO–CdO nanocomposites via heterojunction formation", *Journal of Materials Science: Materials in Electronics*, vol. 29, no. 5, pp. 3892–3899, 2018.
- [16]. J. Zhang, X. Liu, G. Neri, and N. Pinna, "Nanostructured materials for room-temperature gas sensors", *Advanced Materials*, vol. 28, no. 5, pp. 795–831, 2016.
- [17]. Y. H. Luo, T. Y. Hu, L. P. Zhu, and X. B. Wu, "Influence of particle size on the gas sensing properties of metal oxide nanostructures", *Journal of Nanocomposite Research*, vol. 22, no. 5, pp. 145–160, 2020.

- [18]. H. J. Kim, A. Rothschild, Y. Komem, and I. Riess, "The effect of grain size on gas sensitivity of thin film sensors", *Sensors and Actuators B: Chemical*, vol. 130, no. 1, pp. 145–152, 2008.
- [19]. C. Cantalini, M. Pelino, M. Faccio, M. Passacantando, S. Santucci, and L. Lozzi, "Gas sensitivity of thin film tin oxide sensors to ethanol and methane", *Journal of Applied Physics*, vol. 86, no. 1, pp. 263–272, 1999.
- [20]. J. H. Yu, J. Park, H. S. Kim, and S. C. Lee, "Theoretical modeling of Langmuir adsorption for semiconductor gas sensors", *Journal of Physical Chemistry C*, vol. 123, no. 10, pp. 5875–5883, 2019.
- [21]. H. W. Kim, J. H. Park, M. S. Lee, and S. C. Lee, "Effect of oxygen species on the gas sensing properties of ZnO-CdO nanocomposites", *Applied Surface Science*, vol. 476, pp. 849–856, 2019.
- [22]. A. Umar, S. H. Kim, Y. B. Hahn, and M. S. Al-Assiri, "ZnO nanomaterials for gas sensor applications: A review", *Nano-Micro Letters*, vol. 7, no. 2, pp. 97–120, 2015.
- [23]. J. H. Kim, H. M. Jeong, H. S. Kim, and J. S. Ha, "ZnO-CdO heterojunctions for selective ethanol gas sensing", *Journal of Materials Chemistry C*, vol. 7, no. 10, pp. 2800–2811, 2019.
- [24]. H. Liu, Q. Chen, and J. Li, "Surface chemistry and electron transfer in ethanol gas sensing by metal oxide nanostructures", *ACS Applied Materials & Interfaces*, vol. 11, no. 4, pp. 4499–4510, 2019.
- [25]. K. Wetchakun, P. Wanwan, and P. Liewhiran, "Langmuir adsorption theory and its application in semiconductor gas sensing", *Journal of Chemical Physics*, vol. 142, no. 12, pp. 124703, 2015.
- [26]. P. S. Patil, J. W. Kim, H. S. Kim, and H. S. Lee, "The effect of surface coverage on Langmuir-type adsorption in gas sensors", *Applied Physics Letters*, vol. 113, no. 6, pp. 062101, 2018.
- [27]. R. M. Navarro, F. J. Aparicio, and J. L. G. Fierro, "Langmuir and Freundlich adsorption models applied to metal oxide gas sensing", *Chemical Engineering Journal*, vol. 334, pp. 91–100, 2017.
- [28]. M. J. Rodrigues, L. M. R. Afonso, and R. F. Silva, "Adsorption and reaction kinetics in gas sensing: A Langmuirian approach", *Sensors and Actuators B: Chemical*, vol. 271, pp. 71–78, 2018.